RESEARCH   **Open Access**

Functional MRI in the pre-operative assessment of GI-RADS 3, 4, and 5 ovarian masses

Rania S. M. Ibrahim[1*], Manar A. E. L. O. Maher[1], Solava Abdalaziz[2], Samar Amer[2], Doaa Shafie[3] and Soha T. Hamed[1]

Abstract

Background: Characterization of an ovarian lesion is a diagnostic challenge. A correct preoperative assessment is of great importance so as to arrange adequate therapeutic procedures. The aim of the current study is to evaluate the diagnostic performance of functional MRI in differentiation between malignant, borderline, and benign ovarian masses.

Results: This study included 56 adnexal lesions. Bilateral synchronous ovarian lesions are detected in 16 cases. Postoperative histologically proved to be benign in 17 (30%), borderline (low potential malignancy) in 12 (22%), and malignant in 27 (48%). The overall diagnostic performance of conventional MRI in the diagnosis of adenexal lesion was a sensitivity of 74%, specificity of 47%, positive predictive value (PPV) of 76%, negative predictive value (NPV) of 44%, and an accuracy of 66%. Functional pelvic MRI examination showed an increase in overall diagnostic performance compared to conventional values with the highest sensitivity of 90% and NPV of 67% using DWI, and the highest specificity of 88%, PPV of 94%, and an accuracy of 82% using DCE MRI.

Conclusion: Functional MRI in conjugation with conventional MRI plays a key role in the ovarian lesion detection, characterization, and staging. Functional MRI is currently being evaluated as possible predictive and prognostic biomarkers in ovarian lesions.

Keywords: Functional MRI, Ovarian masses, Preoperative, GI-RADS

Background

Ovarian lesions are a typical finding in daily clinical practice. Characterization of an ovarian lesion is a diagnostic challenge. A correct preoperative assessment is of great importance so as to arrange adequate therapeutic procedures [1]. Borderline ovarian tumors (BOTs), or low malignant potential tumors, represent 10–15% of all epithelial ovarian malignancies. BOTs are characterized by the absence of stromal invasion [2]. Preoperatively, BOTs are usually probable to be either benign or malignant ovarian masses, but staging is performed surgically [3]. The diagnosis of BOT can be suggested by the presence of

certain symptoms, serum markers, and image techniques patterns, because CA-125 can overlap between patients with stage I ovarian carcinoma or benign adnexal masses like endometriomas, abscesses, or myomas and BOT patients; therefore, Ca-125 is not helpful in the diagnosis. It can be used in the follow-up and to assess the severity of the disease [4]. The Gynecology Imaging Reporting and Data System (GI-RADS) for adnexal masses was developed by Amor et al. in 2009 and a suggested management protocol was based on the risk of malignancy as estimated by GI-RADS classification (Table 1) [5].

Pelvic and transvaginal ultrasonography (TV-US) is the first-line imaging modality for adnexal lesions and is a particularly useful preoperative test to distinguish benign from malignant conditions. Magnetic resonance imaging (MRI) is of great help in identifying malignant lesions before surgery, particularly when US findings are

* Correspondence: raniasaberm@hotmail.com
[1]Radiology Department (Women's Imaging Unit), Faculty of Medicine, Kasr El-Ainy Hospital, Cairo University, Kasr Al-aini Street, Al-manial District, Cairo, Egypt
Full list of author information is available at the end of the article

Table 1 The GI-RADS classifications [3]

Classification	Morphological features	Risk of malignancy, %	Clinical management
GI-RADS 1	Normal ovaries identified and no adnexal mass seen	0	NA
GI-RADS 2	Classic appearance of functional origin cyst (e.g. follicle, corpus luteum, or hemorrhagic cyst)	<1	Assumed to be functional; requires follow-up by sonography
GI-RADS 3	Classic appearance of common benign neoplasms of the ovary (e.g. teratoma, endometrioma, or paraovarian cyst)	1–4	Assumed to persist over time; surgery required (preferably laparoscopy)
GI-RADS 4	Adnexal lesion not included in GI-RADS 1–3, and with 1–2 morphological findings suggestive of malignancy.★	5–20	Appropriate additional imaging techniques (computed tomography or magnetic resonance imaging); surgical management
GI-RADS 5	Adnexal masses with ≥3 morphological findings suggestive of malignancy	>20	Appropriate additional imaging techniques (computed tomography or magnetic resonance imaging); surgical management

Abbreviations: GI-RADS, Gynecology Imaging Reporting and Data System; NA, not applicable.

GI-RADS Gynecology Imaging Reporting and Data System, *NA* not applicable

★ Morphological findings suggestive malignancy: The presence of wall thickness > 3mm, solid vegetation more than 1cm, thick septa > 3mm, areas of necrosis and breaking down, signs of tumor spread.

Morphological findings suggestive of malignancy: the presence of wall thickness ˃ 3 mm, solid vegetation more than 1 cm, thick septa > 3 mm, areas of necrosis and breaking down, and signs of tumor spread

suboptimal or indeterminate [6]. Functional MRI techniques such DW-MRI, DCE-MRI, and MRS are currently being evaluated as possible predictive and prognostic biomarkers in the context of ovarian malignancy and may play a larger role in routine clinical practice in the future [7].

Methods

This is a prospective study that included 56 ovarian lesions in 40 patients (16 cases showed bilateral masses). They presented with adnexal masses based on preliminary ultrasound examination. We included the cases that fulfilled the following inclusion criteria: complex solid/cystic patterns, vegetations and/or septations in cystic masses, heterogeneous cystic masses, and a large mass size (≥ 5 cm in max. length). We excluded the patients with classical appearance of functional ovarian cyst and any contraindications for MRI. The patients were referred from the Gynecology Department to the Radiology Department (Women's Imaging Unit) during the period from August 2016 to August 2018. All patients or patients' guardians were counseled and signed a consent form. This study was approved by the Radiology Department Kasr Alaini Cairo University hospital research ethics committee. All the patients were investigated for renal function (serum creatinine, urea level, and urine analysis). MRI was performed on two devices (Entra and Achieva, Philips medical system) using a 1.5-T magnet (Table 2). Then they were imaged in the supine position with the aid of pelvic phased-array coil. All patients should be fasting for 3 h and voiding urine 2 h prior examination. Conventional MRI T1 and T2 WI were taken. All lesions were examined according to their size, side (uni- or bilateral), signal intensities, morphological features (predominantly cystic, mixed solid and cystic, and predominantly solid), the presence of papillary projections, solid mural nodules, and associated findings (as ascites, lymphadenopathy and peritoneal deposits). Malignant criteria included the presence of wall thickness ˃ 3 mm, solid vegetation more than 1 cm, thick septa > 3 mm, areas of necrosis and breaking down, and signs of tumor spread for staging: enlarged lymph nodes with lost fatty hilum, ascites, and peritoneal and omental deposits [8]. Borderline masses have also malignant features with thick septations and vegetations; however, they lack the invasive behavior and they were not typical to place them with confidence into either the benign or malignant category, even after a thorough interrogation with the routine MR examination. DW-MRI was done in the axial plane using a single-shot echo-planar imaging sequence at different b values. DCE-MRI was done in all patients, and post-contrast T1 fat sat THRIVE images were obtained immediately after being injected with gadolinium at a dose of 0.1 mmol/kg of body weight (maximum, 20 mL). We calculated the values of the maximum intensity (SI_{max}), maximum relative enhancement (MRE%), wash in rate (WIR), and time to peak (T_{max})

Table 2 MR imaging parameters

Sequence	TR (ms)	TE (ms)	FOV (mm)	Matrix	Slice thickness (mm)	Slice gap (mm)
T2 sagittal	3000	90	290 × 290	208 × 205	4	1.5
T2 axial	3300	100	288 × 350	292 × 180	6	1.3
T1 axial	500	10	260 × 216	263 × 171	6	1.3
T1 SPIR axial	530	8	240 × 240	240 × 190	6	1.3
DWI (*b* = 0, 500, 1000, 1500)	5000	77	240 × 240	124 × 100	6	1
T2 coronal	5000	90	300 × 300	272 × 200	5.5	1
THRIVE	2.8	9.0	370–400	512 × 192	1.5	1
T1 axial post contrast	500	10	260 × 216	263 × 171	6	1.3
T1 coronal post contrast	420	10	280 × 280	256 × 220	6	1
MRS	2000	144/288				

Slice gap is 1 mm and flip angle 90 in all non-contrast sequences

within the most enhancing area of the solid component of the ovarian lesions. Finally, axial, sagittal, and coronal T1-weighted gradient-echo images were acquired. MRS was performed; we assessed the metabolites' peaks in only 32 cases with 40 lesions (8 cases had bilateral lesions) because it is lengthy; and it was refused by other patients. We used multi-voxel point resolved surface coil spectroscopy for volume localization with TE (144 and 288 ms), number of excitations = 6, and interpolated voxel $5 \times 5 \times 5 \text{ mm}^3$. Spectral reconstruction was performed using Phillips advantage windows workstation with functional tool software. MR image interpretation was performed by two double-blinded qualified consultants of radiology (R.I. and S.T, not less than 10 years of experience in pelvic MR imaging).

Statistical analysis

All patients' imaging results were compared with the histopathological diagnosis after surgery. Data was coded and entered using the statistical package SPSS version 15. Data was summarized using number and percent for qualitative variables and mean and standard deviation for quantitative variables. Comparisons between groups were done using chi-squared tests for qualitative variables while quantitative variables are not normally distributed using non-parametrical Mann-Whitney test. Recessive operating characteristic curve was done to test the validity of conventional MRI, the DWI, DCE, and MRS parameters to discriminate between benign, borderline, and malignant lesions. *P* values ≤ 0.05 were considered as statistically significant.

Results

This study included 56 ovarian lesions in 40 patients (16 cases showed bilateral masses). The patients' age ranged from 14 to 75 years old (Mean age 45 +/− 16.073 SD). The adnexal masses were categorized based on preliminary ultrasound examination; we found 15 lesions were

classified as GI-RADS 5, 20 lesions were classified as GI-RADS 4, all of GI-RADS 4–5 lesions were found malignant by conventional and functional MRI, and 21 lesions were classified as GI-RADS 3 which in MRI showed an overlap between borderline/benign lesions. The examined lesions were classified according to the pathological findings (Table 3) (17 (30.5%) benign, 12 (21.5%) borderline, 27 (48%) malignant). Benign lesions (17 lesions) included 6 serous cystadenoma (Fig. 1), 1 mucinous cystadenoma, 7 tubo-ovarian abscesses (TOAs), 2 broad ligament fibroids (Fig. 2), and 1 chronic ectopic pregnancy. Borderline lesions (12 lesions) were 11 borderline papillary serous cystadenoma (Fig. 3) and 1 borderline papillary mucinous cystadenoma. Malignant lesions (27 lesions) included 12 papillary serous cystadenocarcinoma (Fig. 4), 7 mucinous cystadenocarcinoma, 2 granulose cell tumors (Fig. 5), 2 dysgerminoma, 2 endometroid, and 2 malignant Brenner tumors.

By *conventional MRI*, the lesions were examined (Table 4). By *DCE-MRI*, the enhancement patterns of the lesions were detected, and we classified them into the following: benign lesions (17), 15 lesions were predominantly cystic; 6 serous tumors elicited low signal on T1 and high on T2 with mild post-contrast enhancement of their walls and their septae. However, one of them showed focal anterior wall thickening of about 8 mm thickness, showing mild post-contrast enhancement, thus suggesting borderline pathology based on conventional findings; however, it was proven as serous cystadenoma. One mucinous tumor elicited low T1 and high T2 signals but showed fine internal septations. Seven tubo-ovarian complex lesions demonstrated multilocular appearance. They elicited low T1, high T2 signals, incomplete septations, and thickened walls and showed intense post-contrast enhancement, yet blurring of the surrounding fat planes was evident in one lesion. One chronic ectopic pregnancy showed predominantly cystic lesion with internal fine mural nodules < 3 mm and

Table 3 The different final pathological types of the examined lesions

	Benign (n = 17, 30%)	Borderline (n = 12, 22%)	Malignant (n = 27, 48%)
• Epithelial	Mucinous = 1 (5.8%) Serous = 6 (35%)	Serous = 11 (91.6%) Mucinous = 1 (8.3%)	Malignant Brenner tumor = 2 (7.4%) Mucinous = 7 (25.9%) Serous = 12 (44.4%) Endometroid = 2 (7.4 %)
• Sex cord stromal			Granulosa cell tumor = 2 (7.4%)
• Germ cell			Dysgerminoma = 2 (7.4 %)
• Inflammatory	Tubo-ovarian abscess = 7 (41%)		
	Broad ligament fibroid = 2 (11.7%)		
	Chronic ectopic pregnancy = 1 (5.8%)		

showed enhancement of the wall and the fine mural nodules in the post-contrast series. The last two benign lesions were solid; they were diagnosed as broad ligament fibroid (Fig. 2). They demonstrated heterogeneous signal in T1 WIs and low T2 signal. They also showed heterogeneous enhancement in the post-contrast series. BOTs (12) included 11 lesions were predominantly cystic with thick/thin enhancing septations. The last one lesion was cystic tumor with multiple small vegetations measuring between 0.7 and 1.5 cm and eliciting low signal on T1 and high T2 signals with moderate post-contrast enhancement. Malignant tumors (27) included four out of 27 were solid and were pathologically proven as (2) granulosa cell tumor and (2) dysgerminoma. The former elicited low signal on T1 and high signal on T2, with small internal cystic areas, likely of breaking down with intense enhancement on the post-contrast series. One of the granulose cell tumors showed internal areas of high T1 signal likely hemorrhagic. The dysgerminoma tumors showed mixed (intermediate/bright) T2 signal and low T1 signal with heterogeneous post-contrast enhancement. Seventeen out of 27 malignant were mixed solid and cystic lesions (11 lesions of papillary serous cystadenocarcinoma, six lesions of mucinous carcinoma); they demonstrated large solid components eliciting low T1 and high T2 signals with heterogeneous enhancement in the post-contrast series. Six lesions were predominantly cystic: two malignant Brenner's tumor, one papillary serous cystadenocarcinoma, one mucinous cystadenocarcinoma, and two endometroid carcinoma. Associated findings included three benign lesions (5.3 %) and 15 (26.7 %) malignant lesions had mild to moderate ascites. Five (9%) malignant lesions had pelvic and para-aortic lymph nodes. Two malignant lesions (3.5%) had peritoneal nodules. The diagnostic performance in this study used conventional MRI findings; the sensitivity was 74%, specificity was 47%, PPV was 76%, NPV was 93.3%, and accuracy was 66%.

Regarding the *diffusion MRI* findings: (a) Qualitative assessment: The signal intensity of the different ovarian lesions was assessed in DWI different *b* values and corresponding ADC maps, 70% of the lesions showed restricted diffusion (hyper-intense signal in DWI and hypo-intense in ADC map), whereas 30% displayed facilitated diffusion. We also found that 10 out of 17 benign lesions (58.8%) showed restricted diffusion while the remaining showed facilitated diffusion (41.2%), two of the borderline lesions (*n* = 2, 16.6%), whereas all the malignant lesions (*n* = 27, 100%) showed restricted diffusion. (b) Quantitative assessment (ADC values): We found that the cystic components of the tubo-ovarian abscess cases displayed restricted diffusion with very low ADC values in comparison to the rest of the benign lesions. Their values ranged from 0.4 to $0.8 \times 10^{-3} \, \mathrm{mm^2/s}$ with mean value of 0.5345×10^3 (+/− 0.167SD) $\mathrm{mm^2/s}$ (Table 5).

Combining *conventional MRI and DWI* compared to conventional MRI only has increased sensitivity from 74% to 89%, PPV from 76% to 78%, NPV from 44% to 64 %, and accuracy from 66% to 75%, yet the specificity was decreased after adding DWI from 47% (with the use of conventional MRI only) to 41%.

DCE-MRI Findings: (a) Qualitative assessment (the type of curve): We assessed the time intensity curves. Three types of curve existed: type I curve was detected in (13/56) 23.2 %, while type II curve was in (25/56) 44.6% and type III curve was in (18/56) 32% of the lesions (Table 6). (b) Quantitative assessment and cutoff values of the DCE parameters were chosen for the differentiation between benign versus borderline and invasive malignant lesions (Table 7). Combining *conventional MRI and DCE-MRI* compared to conventional MRI only has increased sensitivity from 74% to 79%, specificity from 47% to 88% , PPV from 76% to 94%, NPV from 44% to 65%, and accuracy from 66% to 82%.

In our study, some cases showed discrepancy between the MRI, DWI, and DCE-MRI in their diagnosis:

- Seven proven benign masses were faulty diagnosed malignant by conventional MRI (two broad ligament fibroid, one serous cystadenoma, three TOAs, and one chronic ectopic pregnancy), 5 lesions proven
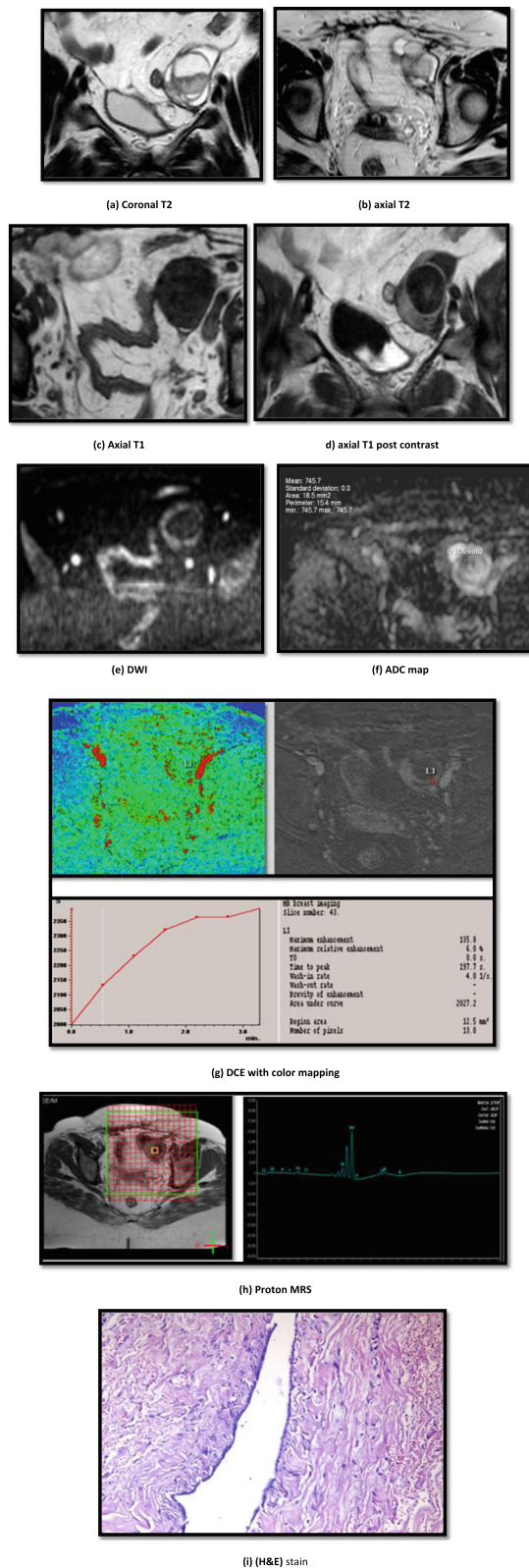
(a) Coronal T2

(b) axial T2

(c) Axial T1

d) axial T1 post contrast

(e) DWI

(f) ADC map

(g) DCE with color mapping

(h) Proton MRS

(i) (H&E) stain

Fig. 1 A 42-year-old-female presented with menstrual irregularity, and pelvic discomfort. US revealed left small multi-locular predominantly cystic lesion with internal septations and solid component (GI-RADS 4). CA-125 was normal. **a–d** Conventional MRI. **a–c** coronal T2, axial T2, and axial T1-weighted images show left multi-locular predominantly cystic adnexal lesion (6 cm), it elicits mixed (intermediate/hyperintense) T2 signal and low T1 signal, it shows multiple internal septations and solid components which show avid enhancement in the post contrast series (**d**). Conventional MRI: Findings are suggestive of a borderline ovarian tumor. **e**, **f** Diffusion WI and ADC map demonstrate diffusion restriction of the solid component of the solid with estimated ADC value measures 0.74×10^{-3} mm^2/s. **g** DCE with color mapping shows type I curve: slowly rising curve. MRE%, 6%; T_{max}, 197.7 s; WIR, 4. **h**, **i** Proton MRS at intermediate TE (144 ms): The spectrum shows high choline peak of its solid components, high NAA peak, and small lipid and lactate peaks. Cho/Cr, 1.5. Multiparametric MRI diagnosis: Findings are suggestive of a left borderline ovarian lesion by conventional MRI, DWIs, and benign curve on DCE-MRI. Operative details: Left salpingo-oophorectomy. **i** H&E stain with original magnification power 25 revealed a cyst with a fibrous wall, lined by a single layer of bland-looking serous cells. Final pathological diagnosis: Left serous cystadenoma (benign epithelial tumors)

borderline cases were faulty diagnosed as malignant (4 serous and 1 mucinous), and only one malignant mass was misdiagnosed as benign (granulose cell tumor).

- Ten benign masses were misdiagnosed by the DWI as malignant; these masses were broad ligament fibroid (*n* = 2) (Fig. 2), chronic ectopic pregnancy (*n* = 1), serous cystadenoma (*n* = 1) (Fig. 1), and TOAs (*n* = 6), whereas two borderline cases were misdiagnosed by the DWI as malignant (two serous tumors) (Fig. 3).

- For DCE-MRI, about 9 malignant masses showed type II curve (Table 6) (2 dysgerminoma, 2 granulosa cell tumor (Fig. 5), and 5 serous cystadenocarcinoma).

MRS Findings: (a) Qualitative assessment: We assessed the metabolites' peaks in 32 cases with 40 lesions (8 cases had bilateral lesions): 16 benign, 2 borderline, and 22 malignant lesions. Choline (cho) peak was present in 32 lesions (76%), including 10 benign (62.5%), 22 malignant (100%), and 2 borderline (100%) lesions. *N*-Acetyl aspartate (NAA) was present in 30 lesions out of the 40 (85%), including 10 benign (62.5%), 1 borderline (50%), and 19 malignant (86.3%) lesions. (b) Quantitative assessment: The metabolite peaks and the mean Cho/Cr ratios were calculated for every pathological group (Tables 8 and 9).

Discussion

The fifth leading cause of cancer death among women is ovarian cancer. It is a disease of post-menopausal women and sometimes prepubescent girls. Risk factors
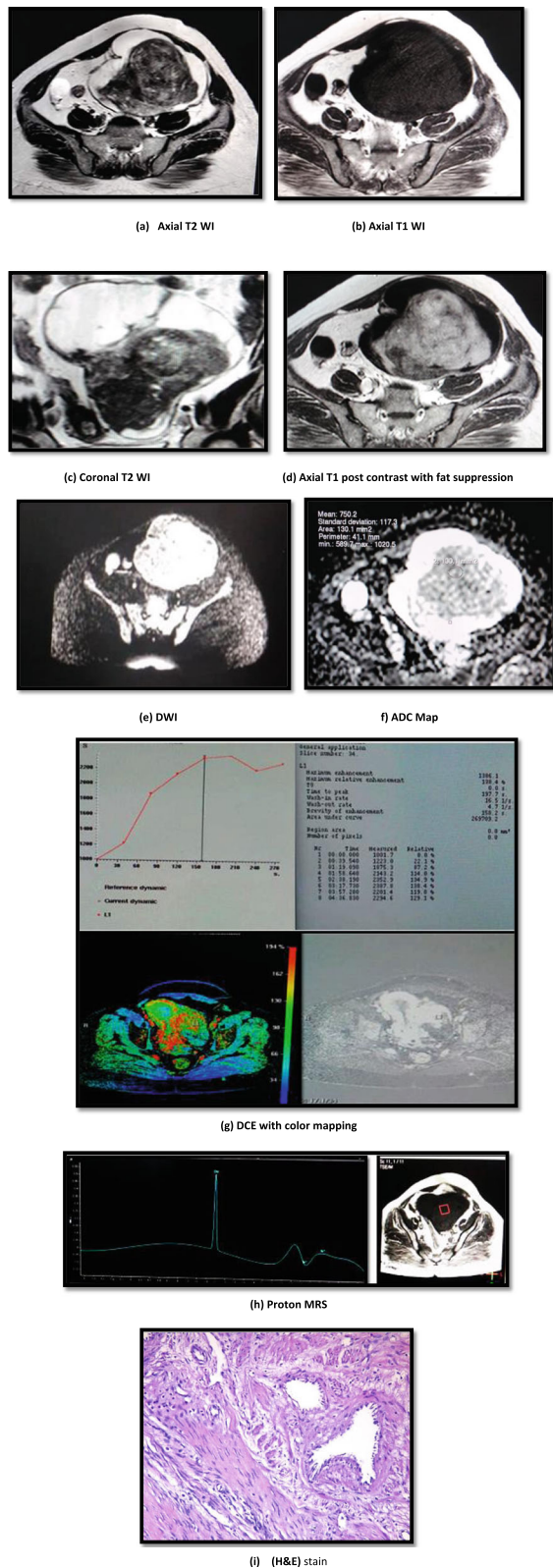
(a) Axial T2 WI

(b) Axial T1 WI

(c) Coronal T2 WI

(d) Axial T1 post contrast with fat suppression

(e) DWI

f) ADC Map

(g) DCE with color mapping

(h) Proton MRS

(i) (H&E) stain

Fig. 2 A 37-year-old female presented with pelvic pain, urine incontinence, and menorrhagia. US revealed left complex (solid/cystic) adnexal lesion (GI-RADS 5). CA-125 was normal. **a–d** Conventional MRI: **a–d** axial T2, axial T1, and coronal T2-weighted images depict a large left adnexal predominantly solid lesion; it measures 17 cm with peripheral cystic area. It elicits low T1 and mixed T2 signals (intermediate/hyperintense). **d** Post-contrast fat suppression axial T1 WI shows intense heterogeneous enhancement of the solid component. **e**, **f** Diffusion WIs and ADC map demonstrate diffusion restriction of the solid component. ADC value measures 0.75×10^{-3} mm^2/s. **g** DCE and color mapping: DCE shows type I curve, slowly raising curve. MRE%, 138.4%; T_{max}, 197.7 s; WIR, 16.5. **h** Proton MRS at intermediate TE (144 ms): the spectrum shows sharp choline peak is observed around 3.2 ppm, small lactate peak is observed around 1.5 ppm, and absent NAA peaks, Cho/Cr ratio = 0.3. Conventional and multiparametric MRI diagnosis: Dynamic contrast MRI suggests benign nature of the lesion. Operative details: the patient was treated by myomectomy. **i** H&E stain with original magnification power 40 revealed a benign smooth muscle tumor formed of interlacing bundles of smooth muscles with fibro-vascular stroma. The muscle cells are spindle cells, with abundant eosinophilic cytoplasm and rod-shaped nuclei. Final pathological diagnosis: Left broad ligament fibroid

include age more than 50, positive family history, infertility, and previous cancer [9]. This study included 56 ovarian lesions in 40 patients (16 cases showed bilateral masses). The patients' age ranged from 14 to 75 years old (mean age 45 +/− 16.073 SD).

Ovarian masses are commonly seen in clinical practice and may be incidentally detected in symptomatic patients. Characterization of an ovarian lesion represents a diagnostic challenge; it is of great importance in the preoperative assessment in order to plan adequate therapeutic procedures and may influence the patient's management [1]. US is the first-line imaging modality for adnexal lesions and is a useful preoperative test for the characterization of noncomplex masses. MRI may be of great help in identifying malignant lesions before surgery, particularly when US findings are suboptimal or indeterminate [6]. In this study, we analyzed the diagnostic performance for the pre-contrast MR sequences, DWI, DCE-MR imaging, and MRS in the evaluation of adnexal masses. We found 15 lesions (26.8%) were classified as GI-RADS 5, 20 lesions (35.7%) were classified as GI-RADS 4, all of GI-RADS 4–5 lesions were found malignant by conventional and functional MRI, and 21 lesions (37.5%) were classified as GI-RADS 3 which in MRI showed an overlap between borderline/benign lesions.

DW-MRI is an important technique that enables the radiologist to move from morphological to functional assessment of diseases of the female pelvis [10]. In this study, 70% of the lesions showed restricted diffusion (hyper-intense signal in DWI and hypo-intense in ADC map), whereas 30% displayed facilitated diffusion. All the malignant (n = 27, 100%) and two of the borderline
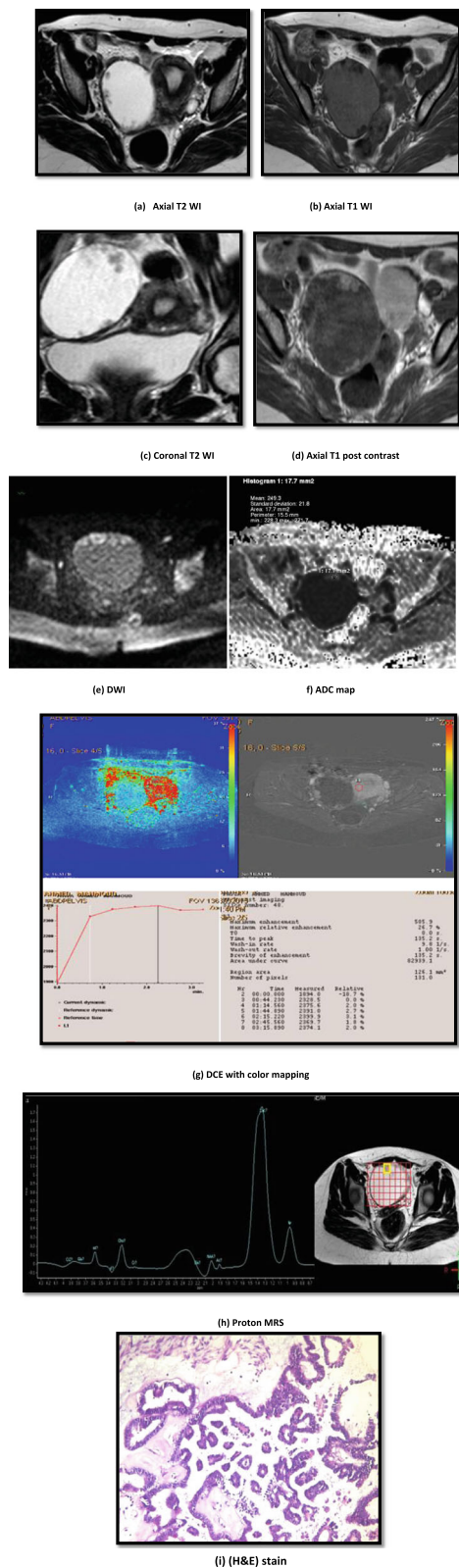
(a) Axial T2 WI   (b) Axial T1 WI

(c) Coronal T2 WI   (d) Axial T1 post contrast

(e) DWI   f) ADC map

(g) DCE with color mapping

(h) Proton MRS

(i) (H&E) stain

Fig. 3 A 36-year-old female presented with chronic pelvic pain. US revealed right predominantly cystic adnexal lesion showing papillary projections (GI-RADS 4). CA-125 was elevated. **a–d** Conventional MRI: **a–c** axial T2, axial T1, and coronal T2 WI depict a large right adnexal predominantly cystic lesion that shows thickened mural nodules. It elicits isointense T1 and high T2 signals. It measures 8 cm. **d** Post-contrast axial T1 WI shows intense post-contrast enhancement of its mural nodules. Conventional MRI findings: Suggestive of a borderline ovarian tumor. **e**, **f** Diffusion WI and ADC map demonstrate diffusion restriction of the mural nodules. ADC value measures 0.24×10^{-3} mm^2/s. **g** DCE with color mapping shows type II curve: initial rapid rise followed by a plateau with delayed washout. MRE%, 26.7%; T_{max}, 135.2 s; WIR, 9.8. **h** Proton MRS at intermediate TE (144 ms): ROI placed within the mural vegetation shows small choline that is observed around 3.2 ppm and NAA peaks and is observed around 2 ppm with a large lipid/lactate peak is observed around 1.3 and 0.9 ppm. Cho/Cr, 0.25. Multiparametric MRI diagnosis: Findings suggest the borderline ovarian tumor. Operative details: right salpingo-oophorectomy. **i** H&E stain with original magnification power 40 revealed an ovarian cyst with papillary projections. The cyst wall and the papillae had fibrous hyalinosed stroma; they were lined by cuboidal cells, with tufting and papillation. The cells showed hypercellularity and low to moderate grade nuclear atypia. No invasion of the cyst wall or the papillary core. Final pathological diagnosis: Right borderline serous tumor

lesions (n = 2, 16.6%), as well as 10 (58.8%) benign lesions that showed restricted diffusion (7 TOAs, 2 broad ligament fibroid, 1 chronic ectopic pregnancy).

Regarding the mean ADC values, we found the solid components for the benign lesions differed significantly from that of the borderline and invasive malignant lesions ($P \leq 0.001$). We conclude that ADC measurement in the solid components was more specific for differentiating benign from malignant lesions; this agrees with a study carried out by Zhang and colleagues [6], they concluded that the presence of a solid component with high or low signal intensity on T2-weighted images and restricted on DWI with low ADC values (less than 1.20×10^{-3} mm2/s) at b = 1000 s/mm2 are predictive of malignancy. However, the presence of a solid component with high or low signal intensity on T2-weighted images and facilitated on DWI being high signal intensity on DWI with high ADC values (greater than 1.20×10^{-3} mm^2/s), or low signal intensity on T2-weighted images and DWI with lower ADC values at b = 1000 s/mm^2 are predictive of benignity.

In contrast, Fujii and colleagues [11] conducted a study on 123 ovarian lesions, recorded that the most malignant ovarian tumors, as well as some of the mature cystic teratomas, and showed high signal intensity on DWI. Also, they concluded that the mean ADC value of the solid portion in malignant tumors did not significantly differ from that in the benign lesions (mean ADC for the benign lesions was 1.47 ± 0.42 and mean ADC for the malignant lesions was 1.41 ± 0.34 ($\times 10^{-3}$ mm^2/

(a) Axial T2

(b) Axial T1

(c) Sagittal T2

(d) T1 Post contrast

(e) DWI

(f) ADC map

(g) DCE with color mapping
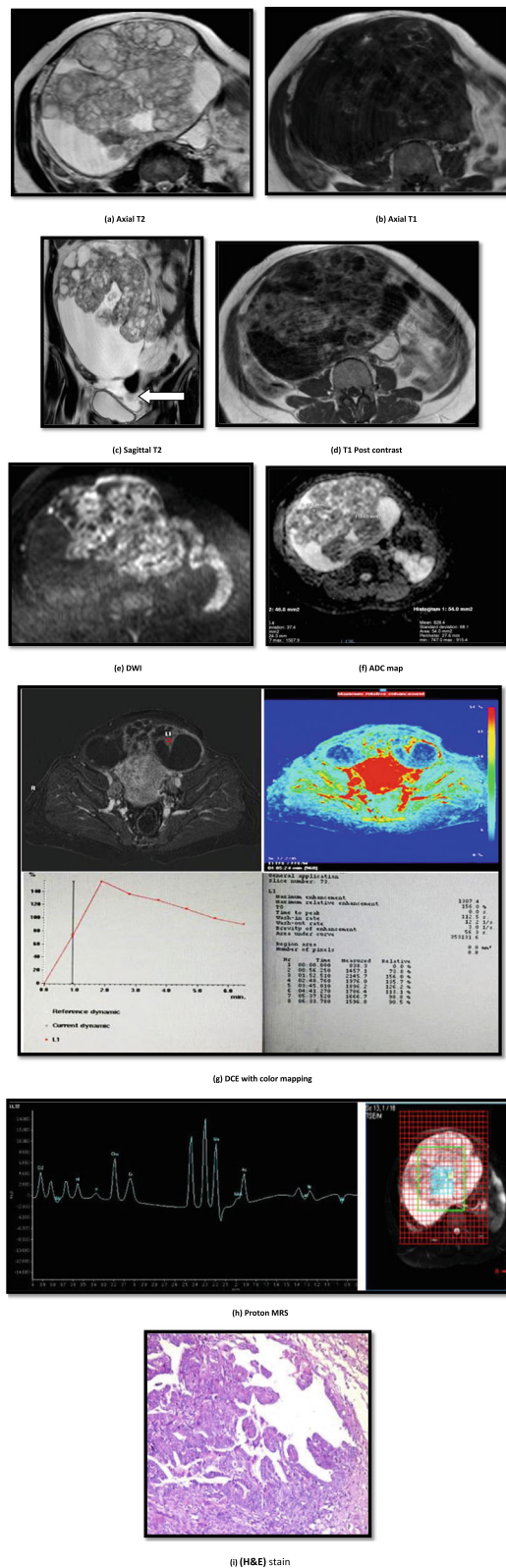
(h) Proton MRS

(i) (H&E) stain

Fig. 4 A 32-year-old female presented with pelvic pain and abdominal distension. US revealed the right large complex adnexal lesion with large solid components and cystic areas (GI-RADS 5). CA-125 was elevated. **a–d** Conventional MRI: **a–c** axial T2, axial T1, and sagittal T2-weighted images show huge right complex (solid/cystic) adnexal lesion; it measures (18.5 cm), it elicits mixed (intermediate/hyperintense) T2 signal and mixed (low/hyperintense) T1 signal, it shows cystic and solid components which show avid enhancement in the post-contrast series (**d**). Pelvic ascites was also noted (white arrow). Conventional MRI findings are suggestive of a malignant ovarian tumor. **e, f** Diffusion WI and ADC map demonstrate diffusion restriction of the solid component of the solid with estimated ADC value measures 0.82×10^{-3} mm^2/s. **g** DCE with color mapping shows type III curve: initial rapid rise with early washout. MRE%, 165%; T_{max}, 112.5 s; WIR, 12.2. **h** at long TE (288 ms): Multi-voxel selected within the solid component of the lesion (**i**) showed large choline peak is observed around 3.2 ppm, and small lactate peak is observed around 1.3 ppm. Cho/Cr, 1.86. Multiparametric MRI diagnosis: Findings are suggestive of right malignant ovarian lesion. **i** H&E stain with original magnification power 40 revealed an ovarian tissue formed of invasive malignant growth and was exhibiting papillary structures. The papillae had thin fibro-vascular cores and lined by malignant serous cells with moderate anaplasia. Final pathological diagnosis: Right high grade invasive papillary serous cystadeno-carcinoma (malignant epithelial tumors)

s)). They attributed this finding to the inclusion of sex cord-stromal tumors, Brenner's tumor, and cyst-adenofibroma, all of which have a dense network of collagen fibers and thus resulting in low ADC values similar to the malignant lesions.

In the current study, also, there was a statistical significance ($P = 0.002$) between the mean ADC values of the cystic components of the benign and borderline/invasive malignant lesions. It may be attributed to the inclusion of the TOA cases which had low ADC values of their cyst contents. All the seven lesions of the TOAs showed diffusion restriction of their cyst contents. Their mean ADC value ranged from 0.6 to 0.8×10^{-3} mm^2/s ($\pm$ 0.19 SD), with a mean value of 0.7×10^3 (+/− 0.16SD) mm^2/s. However, the rest of the benign lesions (which was 1.97 ± 0.428 after the exclusion of the TOAs) showed no significant difference from that of the borderline (1.83 +/− 0.27) or the invasive malignant tumors (2.1 +/− 0.44). This agrees with a study conducted by Wang et al [12] on 69 patients (34 patient with TOA for characterizing the TOA mimicking ovarian malignancy); it showed that the mean ADC value of TOA cystic component was lower than that in malignant tumors (1.04 ± 0 0.41 × 10^{-3} mm^2/s vs. 2.42 ± 0.38 × 10^{-3} mm^2/s; $P < 0.001$).

In our study, the addition of the DWI improved the sensitivity, PPV, NPV, and accuracy of the conventional MRI from 74%, 76%, 44%, and 66% to 89%, 78%, 64%, and 75%, respectively, yet the specificity decreased from 47% to 41%. Such low specificity elicited in our research is explained by the presence of benign cases that have mimicked malignancy on DWI, starting from their
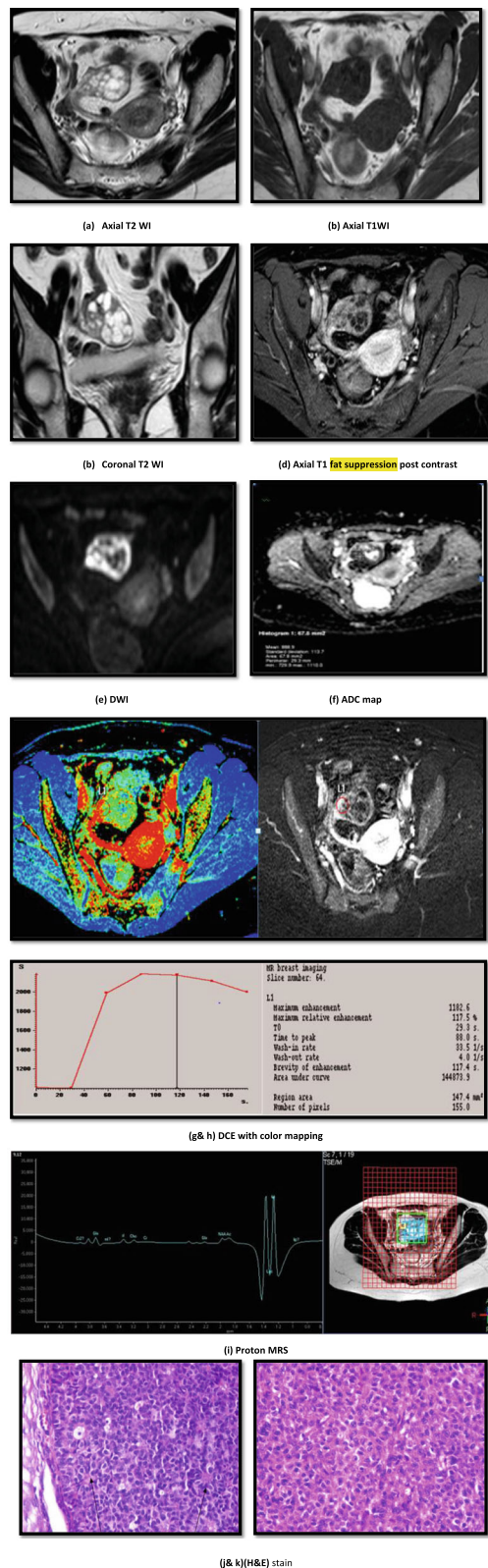
(a) Axial T2 WI

(b) Axial T1WI

(b) Coronal T2 WI

(d) Axial T1 fat suppression post contrast

(e) DWI

(f) ADC map

(g& h) DCE with color mapping

(i) Proton MRS

(j& k)(H&E) stain

Fig. 5 A 39-year-old female patient presented with menometrorrhagia. US was done and revealed small right ovarian lesion. CA-125 was normal. Conventional MRI (**a**–**d**): **a**–**c** axial T2, T1, and coronal T2-weighted images show a right adnexal lesion that shows multiple cystic spaces it measures about 5.5 cm; it elicits low T1 and high T2 signals. The lesion demonstrates intense heterogeneous enhancement with small internal cystic areas of breaking down in post-contrast axial fat suppressedT1 (**d**). Conventional MRI: Findings are suggestive of a benign ovarian tumor regarding its size, signal pattern, absence of septations, vegetations, and mural nodules. **e**, **f** Diffusion WI and ADC map demonstrate diffusion restriction of the solid component of the solid with estimated ADC value measures 0.88×10^{-3} mm^2/s. **g**, **h** DCE with color mapping shows type II curve: initial rapid rise with plateau. MRE%, 117.5%; T_{max}, 88 s, WIR, 33.5. **i** Proton MRS at long TE (288 ms): Spectrum shows a small choline peak, sharp lactate peak, and a small NAA peak. Cho/Cr ratio = 2.2. Multiparametric MRI diagnosis: Findings are in favor of a malignant ovarian tumor. Operative details: Right salpingo-oophorectomy. **j**, **k** H&E stain with original magnification power 25 and 40, respectively, revealed granulosa cell tumor with solid growth showing Call-Exner bodies and coffee-bean nuclei. Final pathological diagnosis: Granulosa cell tumor (malignant sex cord stromal tumor)

misleading signal intensities of restricted diffusion, down to the low ADC values measured; such cases include TOA ($n = 7$), broad ligament fibroid ($n = 2$), and chronic ectopic pregnancy ($n = 1$) showed restricted diffusion due to mixed cellularity of such tumors.

A study done by Mansour et al [13] found that the solo performance of DWI is not an applicable way to discriminate benign from malignant ovarian masses. DWI has high sensitivity and specificity in diagnosing a malignancy in suspicious ovarian masses, provided (1) inclusion of the conventional MRI data, (2) combined analysis of DWI quantitative and qualitative criteria and (3) awareness of the sequence pitfalls. The sensitivity,

Table 4 Summary of conventional MRI findings

Character	Benign	Borderline	Malignant
Number	17 (30%)	12 (22%)	27 (48%)
Mean TS diameters	11.22 cm	7.52 cm	20.025 cm
Side			
Right	8 (47 %)	6 (50%)	9 (33.33%)
Left	7 (41 %)	4 (33.3 %)	6 (22.22%)
Bilateral	2 (11.7%)	2 (16.6%)	12 (44.4%)
Morphology			
Complex cystic	15 (88.2%)	12 (100%)	6 (22.2%)
Mixed	0 (0%)	0 (0%)	17 (62.9%)
Solid	2 (11.7%)	0%	4 (14.8%)
Associated findings			
Ascites	3 (5.3%)	0	15 (26.7%)
Lymph nodes	0	0	5 (9%)
Peritoneal deposits	0	0	2 (3.5 %)

Table 5 The ADC values of both the cystic/ solid components of the adnexal lesions

	Minimum		Maximum		Mean (+/− SD)	
	Cystic	Solid	Cystic	Solid	Cystic	Solid
Benign lesions	0.6	0.7	2.8	1.8	1.55 +/− 0.86	1.12 ± 0.22
Borderline tumors	1.6	0.4	2.5	1.2	1.83 +/− 0.27	0.83 ± 0.34
Malignant tumors	1.2	0.3	2.7	1.1	2.1 +/− 0.44	0.64 ± 0.25

specificity, PPV, NPV, and accuracy of adding DWI to conventional MR imaging was 93%, 85%, 88%, 94%, and 82%, respectively, compared to 93%, 100%, 100%, 92%, and 95% after adding DCE-MRI to the conventional MR.

In contrast to a prospective analysis done by Thomassin-Naggara et al [14], they characterized 77 adnexal masses using DWI. They considered the SI at the DWI to be the accurate tool for predicting benign/malignant criteria, not the ADC values; however, in our study, the ADC value was the most accurate tool.

Challenging cases in our study included (1) TOAs, in which their cystic components showed high signal on the DWI with low ADC values that ranged from 0.6 to 0.8×10^{-3} mm^2/s in the ADC maps, giving a picture similar to a malignant tumor. However, some of those can be diagnosed by detailed clinical history and tumor markers. (2) Broad ligament fibroids, as they demonstrated intermediate to high signals in DWI with low ADC values, fortunately, their iso-intense T1 signals suggested their benign pathology. (3) Ectopic pregnancy, it was predominantly cystic lesion with internal fine mural nodules < 3 mm and showed enhancement of the wall and the fine mural nodules in the post-contrast series and demonstrated high signal in DWI with low ADC values, it was only proven to be ectopic pregnancy only after surgical removal.

We had 12 BOTs that showed variable appearance on DWI. About 10 cases showed facilitated diffusion of its solid component with a high ADC value (1.4×10^{-3} mm^2/s) suggesting benign pathology (false negative). Two cases showed restricted diffusion with high signal on DWI and mean ADC value of 0.6×10^{-3} mm^2/s, suggesting a malignant invasive pathology. Also, borderline

Table 6 Relation of the type of curve to the final pathology

	Pathology			Total
	Benign	Borderline	Malignant	
Curve				
1	7 (41.1%)	6 (50%)	0	13 (23.2%)
2	10 (58.8%)	6 (50%)	9 (33.3%)	25 (44.6%)
3	0 (0%)	0 (0%)	18 (66.6%)	18 (32%)
Total	17 (100.0%)	12 (100.0%)	8(100.0%)	56 (100.0%)

P value, < 0.0001 (significant if < 0.05)

pathology is suggested based on its morphological features "presence of vegetation or thick septations."

Quantitative DCE-MRI provides an accurate method for the prediction of malignancy, particularly in pre-operative indeterminate cases [15]. Sohaib and colleagues [16] described that malignant lesions show greater enhancement than benign lesions during the early phase of enhancement rather than the late phase of enhancement, while benign ovarian tumors showed a gradual increase in enhancement without a well-defined peak, while, borderline ovarian tumors showed moderate initial enhancement followed by a plateau.

Another study carried out by Thomassin-Naggara et al [17] showed that curve type 3 appeared specific for invasive tumors. Curve type 1 was more frequent in benign than in malignant tumors. No difference was found among the three groups (benign, borderline, and malignant) regarding the frequency of curve type 2. However, there was an overlap among the curve types of the benign and borderline lesions; therefore, their capacity to differentiate benign from borderline tumors was low.

In our work, 7 lesions out of 17 benign lesions (41.2%) showed a steady rise with no definite peak (type 1 curve), while the other ten lesions (58.8%) showed a rapid rise with a plateau. Some of the invasive malignant lesions 18 (66.6%) showed an initial rapid steep early enhancement (type 3 curve). However, there was a great overlap between benign and borderline lesions, as we had 6 borderline tumors (borderline serous cystadenomas) which had type 1 curve. We also had 9 cases of malignant tumors which demonstrated type 2 curve (2 bilateral dysgerminomas, 2 mucinous cystadenocarcinomas grade I, 2 granulosa cell tumor, 3 moderately differentiated serous cystadenocarcinoma). Because of the overlap of curve patterns with respect to the histological type, we combined the semi-quantitative parameters.

A study was carried by Kazerooni et al [18] which showed that early enhancement features, i.e. TTP as the most sensitive and WIR as the most specific single classifier, can best describe the properties of ovarian masses, so both have been reported as helpful indicators for discriminating benign and malignant ovarian masses. Therefore, by inspecting DCE-MRI curves in malignant lesions, a steep slope of enhancement, higher WIR, and smaller initial time to enhancement peak can be observed. A study conducted by Li and colleagues [19],

Table 7 The cutoff values of the DCE parameters for the benign& malignant and borderline and malignant adnexal lesions

DCE parameters	Values	Specificity	Sensitivity	PPV	NPV	Accuracy	P value
Borderline and malignant							
SI max	696	71.4	88.2	90.4	60.8	85.7	0.001
MRE	84.78	71.4	81.9	92	49	79.5	0.005
T_{max}	192.65	71.4	91.8	91.2	69.4	85.2	< 0.001
WIR	9.98	71.4	95.9	94.2	84.2	90.6	< 0.001
Benign and malignant							
SI max	990	62.4	90.8	73.8	79.5	78.5	< 0.001
MRE	92	65.8	76.5	65.9	72.4	71.5	0.001
T_{max}	145	84.6	78.7	84.3	83.2	85.4	< 0.001
WIR	12.8	75.9	68.5	82.6	75.7	79.2	< 0.001

Numbers are minimum-maximum (mean +/− SD) (significant if $P < 0.05$)
SI_{max} the maximum intensity, $MRE\%$ maximum relative enhancement, *WIR* wash in rate, and T_{max} time to peak

differentiating malignant and benign ovarian lesions on 48 ovarian tumors (13 benign and 35 malignant) investigated the TTP, produced a sensitivity of 100% and specificity of 92.31%.

In this work, we had found a T_{max} cutoff of ≤ 145 s as predictive of borderline/malignant has produced a maximum statistical significance ($P < 0.001$) with a sensitivity of 78.7% and specificity of 84.6%.

We agreed with a study conducted by Mansour and colleagues [15] on 150 complex or purely solid ovarian masses evaluating the ability of dynamic post-contrast sequence to specify indeterminate ovarian masses, which showed that MRE% was higher for malignant than for benign and borderline masses ($P < 0.001$), but no significant difference was noted between benign and borderline ones ($P > 0.05$).

In this study, we found that MRE% was significantly higher in malignant (mean value of 125.3 ± 54.8 SD) than in benign lesions (mean value 78.25 ± 51.3 SD), and even higher than in borderline lesions (mean value 129 ± 5.2 SD). However, there was some overlap regarding the MRE values between the benign and borderline lesions. However, this can be used to exclude invasive malignancy.

In the study of Bernardin et al [20], calculating mean SI_{max} of the malignant (invasive/borderline lesions) calculated on solid enhancing target components was 712 (278.6 SD), while for benign lesions, it was 491.2 (467.2 SD) with statistical difference ($P = 0.018$).

In our study, using a SI_{max} threshold of ≥ 990 as predictive of malignant invasive pathology gave a sensitivity of 90.8% and a specificity of 62.4%. However, using WIR, we found that the mean value of the WIR in the malignant invasive lesions (19.2 ± 7.4 SD) was much higher than that of the benign (8.17 ± 4.6SD) and borderline (10.3 ± 8.4SD) lesions. Using a WIR cutoff of ≥ 12.8 as predictive of invasive malignant lesions produced a sensitivity of 68.5 % and specificity of 75.9%.

This was in agreement with Bernardin et al [20] that found a statistically significant difference in SI_{max}, SI_{rel}, and WIR between borderline and invasive malignant tumors. Applying a cutoff WIR ≥ 9.5 as predictive of borderline/invasive malignancy produced optimal diagnostic

Table 8 The mean values of the choline/creatine ratio

	Minimum	Maximum	Mean (+/− SD)
Benign	0.02	1.5	0.65 +/− 0.34
Borderline	0.4	0.8	0.63 +/− 0.15
Malignant	0.25	2.5	1.294 +/− 0.98

P value 0.001 (significance < 0.05)

Table 9 Summary of the detected metabolite peaks within the different ovarian lesions

	CHO	NAA	Mean Cho/ Cr	
			Cyst	Solid
Benign (*n* = 16)				
Mucinous cystadenoma (*n* = 1)	+	+	0.47	−
Serous cystadenoma (*n* = 6)	+	+	0.34	−
Broad ligament fibroid (*n* = 2)	−	−	-	1.5
Abscess (*n* = 7)	+	+	0.75	−
Borderline (*n* = 2) (1 serous, 1 mucinous)	+	+	0.45	−
Malignant (*n* = 22)				
Serous cystadenocarcinoma (*n* = 10)	++	+	−	1.56
Mucinous cystadenocarcinoma (*n* = 6)	++	+		2.2
Dysgerminoma (*n* = 2)	+	+	−	1.8
Brenner's tumor (*n* = 2)	+	+	−	2
Granulosa cell tumor (*n* = 2)	+	+	−	2.2

− indicates signal not detected above baseline noise level, + signal detected above baseline noise level, and ++ twofold higher than the average noise level

performance providing a sensitivity of 67% and specificity of 88%.

The TOA were such challenging cases with the use of DCE parameters as they had high MRE% and WIR data (mean values 97.3 ± 52.5 SD and 16.6 ± 4.4 SD, respectively), they had a mean T_{max} 210.8 ± 68.3. Applying a T_{max} threshold of ≤ 145, we had three cases of tubo-ovarian complexes that remained indeterminate. However, fortunately, these types of lesions can be easily diagnosed based on conventional MRI and diffusion findings.

So based on the DCE findings in our work, T_{max} and WIR had the best results showing the highest sensitivity and specificity among the other DCE criteria, along with the type curve. Although DCE-MRI has high specificity for depicting invasive lesions, there was no statistical significance between the benign and borderline lesions regarding the DCE parameters ($P > 0.05$).

DCE-MRI techniques are also prone to pitfalls. False-negative results may occur with poorly vascularized malignant tumors, and false-positive enhancement characteristics may be seen in benign lesions with a high blood supply, such as tubo-ovarian abscess, which may appear complex and indeterminate with all imaging modalities [21].

Molecular imaging through MRS can detect metabolic features characteristic of malignancy. As molecular changes often precede morphologic alterations, sensitivity is expected to improve by MRS [22].

A study conducted by Malek et al [23] on 23 ovarian masses showed the presence of choline peak in 17 of 19 malignant masses (sensitivity 89%) and in 3 of 4 benign masses. So they considered that it could not be used in differentiating between benign and malignant tumors.

In our study, we assessed the metabolites' peaks in 40 lesions. Choline peak was detected in 32 lesions (80%), including 10 out of 16 (62.5%) benign lesions (4 out of 6 abscesses, mucinous, and serous cystadenomas). It was above the noise level but lower than twofold. Two borderline (100%) lesions and 22 malignant (100%) with sharp peaks were found in serous and mucinous cystadenocarcinomas.

This agreed with a study conducted by El Sorogy et al [22] showed Cho peak was detected in all cases of solid tumor or solid parts in cystic tumors. However, the Cho peak was found even in benign tumors and could not be used for the differential diagnosis between benign and malignant tumors.

A study conducted by Stanwell et al [24] showed a higher Cho/Cr ratio in malignant ovarian cancer than in benign cystic ovarian tumors. Also, a study conducted by El Sorogy et al [22] showed the sensitivity of Cho/Cr ratio in differentiating benign from malignant ovarian lesions was 0.83 and specificity 0.82.

In this study, mean Cho/Cr ratio was 1.29 ± 0.98 SD for malignant lesions, while the mean value in borderline lesions was 0.63 ± 0.15 SD and the mean value for the benign lesions was 0.65 ± 0.34. There was a statistical significance regarding the Cho/Cr ratio between the benign and invasive malignant lesions ($P \leq 0.001$) as well as between the borderline and invasive lesions ($P = 0.05$), but not between the benign and borderline lesions (Table 8).

A study conducted by Stanwell et al [24] reported the presence of NAA in all of the teratomas and serous cystadenomas, as well as a portion of the serous carcinomas. Also, its amplitude was greater in malignant than in benign tumors. Kolwijck et al [25] concluded that both NAA and N-acetyl groups from glycoproteins and/or glycolipids may contribute to the Delta 2.0–2.1 ppm resonance complex in the ovarian cyst fluid.

In our study, we found NAA peaks in serous and mucinous cystadenomas and tubo-ovarian abscesses. NAA peak was also detected in one borderline tumor and most of the malignant tumors (19 lesions).

A study conducted by El Sorogy and colleagues [22] found a very striking finding is that lactate signal was found in almost all benign lesions, and not obtained in any of malignant lesions except dysgerminoma. Another study conducted by MA and colleagues [26] on 69 patients, choline peak was detected in all cases (100%), NAA peak in 67 cases (97%, 25 benign and 42 malignant), lipid peak in 47 cases (17 benign and 30 malignant), and lactate peak in only eight cases (four benign and four malignant).

In our study, sharp lactate peaks were found in serous benign lesions, TOA, broad ligament fibroids, solid portions of the borderline lesions as well as the solid portions of the malignant serous and mucinous cystadenocarcinoma lesions (Table 9).

BOTs are known also as tumors of low malignant potential. They are characterized by atypical epithelial proliferation and moderate nuclear atypia but without stromal invasion. Patients with BOTs generally have an excellent prognosis after surgical excision because they are more likely to present in an early stage; however, they show a high recurrence rate. It is important to preoperatively discriminate BOTs from invasive malignant tumors because a conservative fertility-sparing laparoscopic surgery can be performed in the former [27]. The preoperative diagnosis of BOTs remains challenging regarding the clinical, laboratory, and imaging findings [28]. Morphological imaging features suggesting borderline tumors have been investigated; however, there are overlapping with those of invasive epithelial tumors. So, better imaging tools are needed to improve the distinction of invasive, borderline, and benign adnexal lesions [20].

In our study, BOTs presented a great challenge for us. Their morphological features can mimic benign or malignant lesions, yet they lack the invasive behavior of the malignant lesions. However, in functional imaging, most of them mimic benign lesions, which is consistent with their non-invasive behavior.

Conclusion

- Functional MRI in conjugation with conventional MRI plays a key role in the characterization of indeterminate adnexal lesions. Functional MRI is currently possible predictive and prognostic biomarkers in ovarian lesions.
- Functional MRI helps to discriminate benign ovarian lesions from invasive malignancy and even BOTs from invasive malignancy based on DCE-MRI parameters.
- DWI can confirm or exclude potential malignancy in complex adnexal masses, provided (1) inclusion of the conventional MRI data, (2) combined analysis of DWI quantitative and qualitative criteria, and (3) awareness of the possible sequence pitfalls.
- The addition of MRS to the conventional MRI has markedly improved its diagnostic value. They provide additional information for the tumor behavior. Being non-invasive cost-effective techniques, they are recommended to be added to the routine conventional MRI to help characterization of indeterminate masses. Continuous research for the DCE and MRS should be done to establish optimum diagnostic criteria and to improve their diagnostic value.

Abbreviations
ADC: Apparent diffusion coefficient; BOTs: Borderline ovarian tumors; CHO: Choline; CHO/Cr: Choline/creatine; DCE-MRI: Dynamic contrast-enhanced MRI; DWI: Diffusion-weighted imaging; GI-RADS: Gynecology Imaging Reporting and Data System; MRE%: Maximum relative enhancement; MRS: Magnetic resonance spectroscopy; NAA: *N*-Acetyl aspartate; NPV: Negative predictive value; PPV: Positive predictive value; SI_{max}: Maximum intensity; T_{max}: Time to peak; TOAs: Tubo-ovarian abscesses; TV-US: Transvaginal ultrasonography; WIR: Wash in rate

Authors' contributions
SH contributed to the study concept. SH and RI contributed to the study design. MM contributed to the data acquisition, manuscript preparation, and manuscript editing. MM, RI, and SA contributed to the data analysis and interpretation. RI contributed to the statistical analysis. SH, RS, DSH, and SAA contributed to the manuscript reviewing. All authors have read and approved the manuscript.

Availability of data and materials
The datasets used and/or analyzed during the current study are available from the corresponding author on reasonable request.

Author details
[1]Radiology Department (Women's Imaging Unit), Faculty of Medicine, Kasr El-Ainy Hospital, Cairo University, Kasr Al-aini Street, Al-manial District, Cairo, Egypt. [2]Histopathology Department, Kasr El-Ainy Hospital, Cairo University, Cairo, Egypt. [3]Obestetric and Gynecology Department, Kasr El-Ainy Hospital, Cairo University, Cairo, Egypt.

References
1. Foti PV, Attinà G, Spadola S, Caltabiano R, Farina R, Palmucci S et al (2016) MR imaging of ovarian masses: classification and differential diagnosis. Insights Imaging 7:21–41
2. Alvarez RM, Vicente DV (2015) Fertility sparing treatment in borderline ovarian tumour. Ecancermedicalscience 9:507
3. Cadron I, Leunen K, Van Gorp T, Amant F, Neven P, Vergote I (2007) Management of borderline ovarian neoplasms. J Clin Oncol 25(20): 2928–2937
4. Cormio G, Loizzi V, Falagario M, Scardigno D, Latorre D, Selvaggi LE. Boderline epithelial tumors of the ovary, ovarian cancer- a clinical and translational update, 2013, Chapter 4, p.78:96.
5. Zhang T, Li F, Liu J, Zhang S (2017) Diagnostic performance of the gynecology imaging reporting and data system for malignant adnexal masses. Int J Gynecol Obstet 137:325–331
6. Zhang P, Li W, Chu C, Cui Y, Zhu M (2012) Diffusion-weighted MRI: a useful technique to discriminate benign versus malignant ovarian surface epithelial tumors with solid and cystic components. Abdom Imaging 37: 897–903
7. Vargas HA, Barrett T, Sala E (2013) MRI of ovarian masses. J Magn Reso Imaging 37(2):265–281
8. Valentini AL, Gui B, Micco M, Mingote MC, De Gaetano AM, Ninnivaggi V et al (2012) Suspicious ovarian masses- MR imaging criteria for characterization: pictorial review. J Oncol 481806:1–9. https://doi.org/10.1155/2012/481806
9. Shahid MK, Jamal R, Katherine LC, Monica PH, Linus C, Josef M et al (2011) Role of FDG PET/CT in staging of recurrent ovarian cancer. Radiographics 31:569–583
10. Sala E, Rockall A, Rangarajan D, Kubik-Huch RA (2010) The role of dynamic contrast-enhanced and diffusion weighted magnetic resonance imaging in the female pelvis. Eur J Radiol 76:367–385
11. Fujii S, Kakite S, Nishihara K, Kanasaki Y, Harada T, Kigawa J et al (2008) Diagnostic accuracy of diffusion-weighted imaging in differentiating benign from malignant ovarian lesions. J Magn Reson Imaging 28:1149–1156
12. Wang T, Li W, Wu X, Yin B, Chu C, Ding, Cui Y (2016) Tubo-ovarian abscess (with/without pseudotumor area) mimicking ovarian malignancy: role of diffusion-weighted MR imaging with apparent diffusion coefficient values. PLoS One 11(2):1–17
13. Mansour SM, Saraya S, El-faissal Y (2015) Semi-quantitative contrast-enhanced MR analysis of indeterminate ovarian tumors: when to say malignancy? Br J Radiol 88:1–13
14. Thomassin-Naggara I, Daraï E, Cuenod CA, Fournier L, Toussaint I, Marsault C et al (2009) Contribution of diffusion-weighted MR imaging for predicting benignity of complex adnexal masses. Eur Radiol 19:1544–1552

15. Dogheim OY, Abdel Hamid AM, Barakat MS, Eid M, El Sayed SM (2014) Role of novel magnetic resonance imaging sequences in characterization of ovarian masses. Egypt J Radiol Nucl Med 45(1):237–251
16. Sohaib SAA, Sahdev A, Trappen PV, Jacobs IJ, Reznek RH (2003) Characterization of adnexal mass lesions on MR imaging. AJR Am J Roentgenol 180(5):1297–1304
17. Thomassin-Naggara I, Balvay D, Rockall A, Carette MF, Ballester M, Darai E et al (2015) Added value of assessing adnexal masses with advanced MRI techniques. Biomed Res Int 785206:1–10. https://doi.org/10.1155/2015/785206
18. Kazerooni AF, Malek M, Haghighatkhah H, Parviz S, Nabil M, Torbati L et al (2016) Semiquantitative dynamic contrast-enhanced MRI for accurate classification of complex adnexal masses. J Magn Reson Imaging 45:418–427
19. Li HM, Qiang JW, Ma FH, Zhao SH (2017) The value of dynamic contrast-enhanced MRI in characterizing complex ovarian tumors. J Ovarian Res 10(4):1–7
20. Bernardin L, Dilks P, Liyanage S, Miquel ME, Sahdav A, Rockall A (2012) Effectiveness of semi-quantitative multiphase dynamic contrast-enhanced MRI as a predictor of malignancy in complex adnexal masses: radiological and pathological correlation. Eur Radiol 22(4):880–890
21. Mohaghegh P, Rockall AG (2012) Imaging strategy for early ovarian cancer: characterization of adnexal masses with conventional and advanced imaging techniques. Radiographics 32:1751–1773
22. El sorogy L, Abd El gaber N, Omran E (2012) Role of diffusion MRI and proton magnetic resonance spectroscopy in characterization of ovarian neoplasms. Egypt J Radiol Nucl Med 43:99–106
23. Malek M, Pourashraf M, Mousavi AS, Rahmani M, Ahmadinejad N, Alipour A et al (2015) Differentiation of benign from malignant adnexal masses by functional 3 Tesla MRI techniques: diffusion-weighted imaging and time-intensity curves of dynamic contrast enhanced MRI. Asian Pac J Cancer Prev 16:3407–3412
24. Stanwell P, Russell P, Carter J, Pather S, Heintze S, Mountford C (2008) Evaluation of ovarian tumors by proton magnetic resonance spectroscopy at three tesla. Invest Radiol 43:745–751
25. Kolwijck E, Engelke UF, Van Der Graaf M, Heerschap A, Blom HJ, Hadfoune M et al (2009) N-acetyl resonances in vivo and in vitro NMR spectroscopy of cystic ovarian tumors. NMR Biomed 22:1093–1099
26. Ma FH, Qiang JW, Cai SQ, Zhao SH, Zhang GF, Rao YM (2015) MR Spectroscopy for differentiating benign from malignant solid adnexal tumors. AJR 2004(6):724–730
27. Zhao SH, Qiang JW, Zhang GF, Ma FH, Cai SQ, Li HM et al (2014) Diffusion –weighted MR imaging for differentiating borderline from malignant epithelial tumors of the ovary: pathological correlation. Eur Radiol 24:2292–2299
28. Morotti M, Menada MV, Gillot DJ, Venturini PL, Ferrero S (2012) The preoperative diagnosis of borderline ovarian tumors: a review of current literature. Arch Gynecol Obstet 285:1103–1112. https://doi.org/10.1007/s00404-011-2194-1

Publisher's Note